NUKLEONIKA 2010;55(3):293–302

ORIGINAL PAPER

Nuclear data for the cyclotron production of ^{66}Ga, ^{86}Y, ^{76}Br, ^{64}Cu and ^{43}Sc in PET imaging

Mahdi Sadeghi, Milad Enferadi, Morteza Aref, Hoda Jafari

Abstract. Positron emission tomography (PET) is a powerful diagnostic tool, which provides superior spatial resolution and an opportunity to obtain quantitative information concerning distribution of radioactivity *in vivo*. Most interesting positron emitters for the purpose of diagnose are ^{64}Cu, ^{124}I, ^{18}F, ^{86}Y, ^{48}V, ^{52}Mn, ^{140}Pr, ^{72}As, ^{74}As, ^{89}Zr, ^{82}Sr, ^{68}Ga, ^{66}Ga, ^{45}Ti, ^{76}Br and ^{82}Rb. Aim of the presented study is to compare the calculated cross sections of several radioisotopes of positron emitters as follows ^{86}Y, ^{43}Sc, ^{64}Cu, ^{66}Ga and ^{76}Br with incident proton energy up to 30 MeV. In this work, excitation function of positron emitters via the ^{86}Sr(p,n)^{86}Y, ^{43}Ca(p,n)^{43}Sc, ^{66}Zn(p,n)^{66}Ga, ^{64}Ni(p,n)^{64}Cu and ^{76}Se(p,n)^{76}Br reactions were calculated by ALICE/ASH 0.1 (GDH model and hybrid model) and TALYS-1.2 (equilibrium and pre-equilibrium) codes and compared to existing data. Requisite for optimal thicknesses of targets were obtained by the stopping and range of ions in matter (SRIM) code for each reaction.

Key words: production yields • excitation function • positron emitters • ALICE/ASH • TALYS-1.2

M. Sadeghi✉, H. Jafari
Agricultural, Medical and Industrial Research School,
Nuclear Science and Technology Research Institute,
P. O. Box 31485-498, Karaj, Iran,
Tel.: +98 261 443 6395, Fax: +98 261 446 4055,
E-mail: msadeghi@nrcam.org

M. Enferadi
Faculty of Engineering,
Research and Science Branch,
Islamic Azad University,
Tehran, Iran

M. Aref
Physics Department,
Zanjan University,
P. O. Box: 451-313, Zanjan, Iran

Received: 10 May 2010
Accepted: 13 July 2010

Introduction

^{64}Cu is a useful radiotracer for PET and a promising radiotherapy agent for the treatment of cancer. ^{64}Cu ($T_{1/2}$ = 12.7 h, $E_{\beta^+_{max}}$ = 657 keV) can be used for antibody fragments with slower kinetics, for which imaging the day after injection may be desirable [1, 36, 38, 39, 43, 44]. ^{86}Y ($T_{1/2}$ = 4.7 h, I_{EC} = 66%, I_{β^+} = 34%, $E_{\beta^+_{max}}$ = 1.2 MeV) has been proposed as a PET imaging surrogate to ^{90}Y that is widely applied for unsealed radiotherapy such as treating non-Hodgkins lymphoma, bone pain palliation by the endocrine therapy (ERT) method, treatment of malignant gliomas, Hepatoma, gastrointestinal adenocarcinomas, and rheumatoid arthritis [2, 12, 14, 46, 47].

^{76}Br has a fairly high abundance of positron emission (I_{β^+} = 54%) and a half-life of 16.2 h which is long enough to follow the kinetics of, e.g. antibody distribution during 2 full days. The ^{76}Se(p,n)^{76}Br reaction, using a ^{76}Se-enriched Cu_2Se target, enables a simple and cost-effective routine production of ^{76}Br in a low-energy cyclotron [29, 37, 38, 50, 55]. For labelling antibody fragments, the use of more long-lived ^{66}Ga ($T_{1/2}$ = 9.4 h) might be preferable. Gallium-66 can be produced using the ^{63}Cu(^{4}He,n)^{66}Ga or the ^{66}Zn(p,n)^{66}Ga (isotopically enriched target, energy range from 14.5 to 6 MeV) nuclear reactions. The ^{66}Zn(p,n)^{66}Ga nuclear reaction-based production route is preferable because it can be accomplished using commonly available low-energy cyclotrons [7, 20, 32, 42, 54].

Material and methods

Calculation of excitation function

Excitation functions of ^{86}Sr, ^{43}Ca, ^{64}Ni, ^{66}Zn and ^{76}Se + p reactions were calculated by using ALICE/ASH and TALYS-1.2 codes [24, 25, 27]. The codes were used simultaneously to increase the accuracy of calculations. An optimum energy range was determined and employed to avoid the formation of radionuclide impurities and decrease the excitation functions of inactive impurities as far as possible. To further achieve the aim, feasibility of the production of positron emitters via proton induced per low/medium energy accelerators was investigated.

Nuclear level densities

Investigation of nuclear level densities is of great interest in nuclear physics, since they are of importance both in developing a consistent theoretical description of the properties of excited nuclei and in calculating cross sections for nuclear reactions within the statistical model. Such calculations include investigations into nuclear synthesis in nuclear astrophysics. Since the Bethe model of 1936 some more or less successful phenomenological expressions based, e.g. on the Fermi-gas or the so-called back shifted Fermi-gas model were proposed to reproduce the existing data and predict the not yet measured cases. Theoretical calculations within the shell model and the Monte Carlo (MC) methods, which generally include pairing correlations, and take the influence of spin and parity into account, have been quite successful in this context [4, 8, 10, 34, 35, 56].

The ALICE/ASH code

The ALICE/ASH code is a modified and advanced version of the ALICE code [5]. The geometry dependent hybrid (GDH) model is used for the description of the preequilibrium particle emission. Intra-nuclear transition rates are calculated using the effective cross section of nucleon-nucleon interactions in nuclear matter. Corrections are made to the GDH model for the treatment of effects in peripheral nuclear regions. The number of neutrons and protons for initial exciton state is calculated using realistic nucleon-nucleon interaction cross sections in nucleus. The exciton coalescence model and the knock-out model are used for the description of the preequilibrium complex particle emission. The equilibrium emission of particles is described by the Weisskopf-Ewing model without detail consideration of angular momentum [6, 28, 48, 51].

Nuclear level density in ALICE/ASH 0.1

The level density for equilibrium states is calculated using one of the following approaches.

Fermi gas model with an energy independent level density parameter

The nuclear level density is taken in the form

$$\rho(U) \propto (U-\delta)^{-5/4} \exp(2\sqrt{a(U-\delta)}) \tag{1}$$

and the level density parameter is equal

$$a = A/y \tag{2}$$

where y is a constant. The pairing correction, δ can be evaluated using different schemes depending upon the input parameter *MP*: "standard" shift ($MP = 3$)

$$\delta = 11/A^{1/2} \quad \text{for even-even nuclei,} \tag{3}$$

$$\delta = 0 \quad \text{for nuclei with odd } A, \tag{4}$$

$$\delta = -11/A^{1/2} \quad \text{for odd-odd nuclei} \tag{5}$$

"backshift" ($MP = 1$)

$$\delta = 0 \quad \text{for even-even nuclei} \tag{6}$$

$$\delta = -11/A^{1/2} \quad \text{for nuclei with odd } A \tag{7}$$

$$\delta = -22/A^{1/2} \quad \text{for odd-odd nuclei} \tag{8}$$

At excitation energies below 2 MeV, the level density is calculated by the "constant" temperature model.

Kataria-Ramamurthy Fermi gas model [21]

$$a = \alpha A + \beta_0 A^{2/3} + \beta_1 A^{2/3}/S_n + \beta_2 A^{2/3}/S_p \tag{9}$$

The parameter a is on the basis of a number of model single-particle energy level schemes. Simple functional form for the parameter a was proposed, taken into account the effect of the Fermi energy of nucleons.

The parameters has been obtained by least square fit to the 'experimental' values for spherical nuclides in the mass-region $40 < A < 210$ ($a = 0.08$ MeV^{-1}, $\beta_0 = -0.12$ MeV^{-1}, $\beta_1 = 1.35$, $\beta_2 = 1.4$) [22, 23].

Fermi gas model of Ignatyuk, Smirenkin, Tishin with an energy dependent level density parameter

The nuclear level density is defined by the expression

$$\rho(U) \propto a^{1/4} (U-\delta)^{-5/4} \exp(2\sqrt{a(U-\delta)}) \tag{10}$$

The nuclear level density parameter is calculated as follows [27]

$$a(U) = \tilde{a}\,(1 + f(U)\,\delta W/U) \tag{11}$$

where δW is the shell correction,

$$f(U) = 1 - \exp(-\gamma U) \tag{12}$$

$$\tilde{a} = A(\alpha + \beta A), \tag{13}$$

where $\alpha = 0.154$, $\beta = -6.3 \times 10^{-5}$ and $\gamma = 0.054$ MeV^{-1}. The pairing correction is

$$\delta = 24/A^{1/2} \quad \text{for even-even nuclei} \tag{14}$$

(15) $\delta = 12/A^{1/2}$ for nuclei with odd A

(16) $\delta = 0$ for odd-odd nuclei

At excitation energies < 2 MeV, the level density is calculated using the "constant" temperature approach.

Superfluid nuclear model

The nuclear level density is calculated according to the generalized Superfluid Model [19]

(17) $$\rho(U) = \rho_{qp}(U') K_{vib}(U') K_{rot}(U')$$

where $\rho_{qp}(U')$ is the density of quasi-particle nuclear excitation, $K_{vib}(U')$ and $K_{rot}(U')$ are the vibrational and rotational enhancement factors at the effective energy of excitation U' calculated by Ignatyuk [17].

The nuclear level density parameters are calculated according to the expression [18].

(18) $$a(U) = \begin{cases} \tilde{a}(1+\delta W \varphi)U' - E_{cond}/(U' - E_{cond}), U' > U_{cr} \\ a(U_{cr}), \qquad U' \le U_{cr} \end{cases}$$

where δW is the shell correction to the mass formula equal to the difference between experimental mass defect and the one calculated from the liquid drop model [33]

(19) $$\phi(U) = 1 - \exp(-\gamma U), \ \gamma = 0.4/A^{1/3} \text{ MeV}^{-1}$$

The asymptotic value of nuclear level parameter is equal to

(20) $$\tilde{a} = A(0.073 + 0.115A^{-1/3})$$

The effective energy of excitation U', the critical energy of the phase transition U_{cr} and the condensation energy E_{cond} are calculated as follows:

(21) $$U' = U - n\Delta_0,$$

(22) $$U_{cr} = 0.472\, a(U_{cr})\, \Delta_0^2 - n\Delta_0,$$

(23) $$E_{cond} = 0.152\, a(U_{cr})\, \Delta_0^2 - n\Delta_0,$$

The correlation function Δ_0 is equal to

(24) $$\Delta_0 = 12A^{-1/2}$$

where $n = 0$ for even-even nuclei, $n = 1$ for nuclei with odd A value, $n = 2$ for odd-odd nuclei. The precompound emission was described using the GDH model [6, 26, 49].

The TALYS 1.2 code

TALYS 1.2 code is optimized for incident projectile energies, ranging from 1 keV up to 200 MeV on target nuclei with mass numbers between 12 and 339. It includes photon, neutron, proton, deuteron, triton, ^{3}He, and α-particles as both projectiles and ejectiles, and single-particle as well as multi-particle emissions and fission. All experimental information on nuclear masses, deformation, and low-lying states spectra is considered, whenever available and if not, various local and global input models have been incorporated to represent the nuclear structure properties, optical potentials, level densities, γ-ray strengths, and fission properties. The TALYS code was designed to calculate total and partial cross sections, residual and isomer production cross sections, discrete and continuum γ-ray production cross sections, energy spectra, angular distributions, double differential spectra, as well as recoil cross sections. The preequilibrium particle emission is described using the two-component exciton model. The model implements new expressions for internal transition rates and new parameterization of the average squared matrix element for the residual interaction obtained using the optical model potential [3, 25]. The phenomenological model is used for the description of the preequilibrium complex particle emission. The equilibrium particle emission is described using the Hauser-Feshbach model.

In statistical models for predicting cross sections, nuclear level densities are used at excitation energies where discrete level information is not available or incomplete. Several models use for the level density in TALYS, which range from phenomenological analytical expressions to tabulated level densities derived from microscopic models. To set the notation, first give some general definitions. The level density $\rho(E_x, J, \Pi)$ corresponds to the number of nuclear levels per MeV around an excitation energy E_x, for a certain spin J and parity Π. The total level density $\rho^{tot}(E_x)$ corresponds to the total number of levels per MeV around E_x, and is obtained by summing the level density over spin and parity:

(25) $$\rho^{tot} E(x) = \sum_J \sum_\Pi \rho(E_x, J, \Pi)$$

The nuclear levels are degenerate in M, the magnetic quantum number, which gives rise to the total state density $\omega^{tot}(E_x)$ which includes the $2J + 1$ states for each level, i.e.

(26) $$\omega^{tot} E(x) = \sum_J \sum_\Pi (2J+1)(E_x, J, \Pi)$$

When level densities are given by analytical expressions they are usually factorized as follows

(27) $$\rho(E_x, J, \Pi) = P(E_x, J, \Pi)\, R(E_x, J)\, \rho^{tot}(E_x)$$

where $P(E_x, J, \Pi)$ is the parity distribution and $R(E_x, J)$ the spin distribution. In all but one level density model in TALYS, the parity equipartition is assumed, i.e. [25]

(28) $$P(E_x, J, \Pi) = \tfrac{1}{2}$$

Calculation of the required thickness of target

According to SRIM code the required thickness of target was calculated [57]. The physical thickness of the target layer is chosen in such a way that for a given beam/target angle geometry (90°) the incident beam be exited of target layer with predicted energy. To minimize thickness of the target layer, 6° geometry

Table 1. ^{86}Y, ^{43}Sc, ^{64}Cu, ^{66}Ga and ^{76}Br production yields by SRIM and TALYS-1.2 code

Reaction	Isotopic abundance (%)	Energy range (MeV)	Target thickness (μm)	Theorical field (MBq/μA·h)	*Q*-value (MeV)	*E*-threshold (MeV)
^{86}Sr(p,n)^{86}Y	9.86	13 → 18	73.45	793.90	–6.02	6.092
^{76}Se(p,n)^{76}Br	9.36	12 → 17	49	372.46	–5.74	6.048
^{66}Zn(p,n)^{66}Ga	27.9	9 → 15	61	446.53	–5.95	6.040
^{43}Ca(p,n)^{43}Sc	0.135	6 → 13	220	110.28	–3.003	3.073
^{64}Ni(p,n)^{64}Cu	0.926	8 → 13	101	68.31	–2.457	2.4961

is preferred; so the required layer thickness will be less with coefficient 0.1. The calculated thicknesses were shown for ideal reactions in Table 1.

Calculation of theoretical yield

Enhance of the projectile energy, the beam current and the time of bombardment increase the production yield. The production yield can be calculated as below

$$Y = \frac{N_L H}{M} I(1-e^{-\lambda t}) \int_{E_1}^{E_2} \left(\frac{dE}{d(\rho x)} \right)^{-1} \sigma(E) dE \quad (29)$$

where Y is the product activity (in Bq) of the product, N_L is the Avogadro number, H is the isotope abundance of the target nuclide, M is the mass number of the target

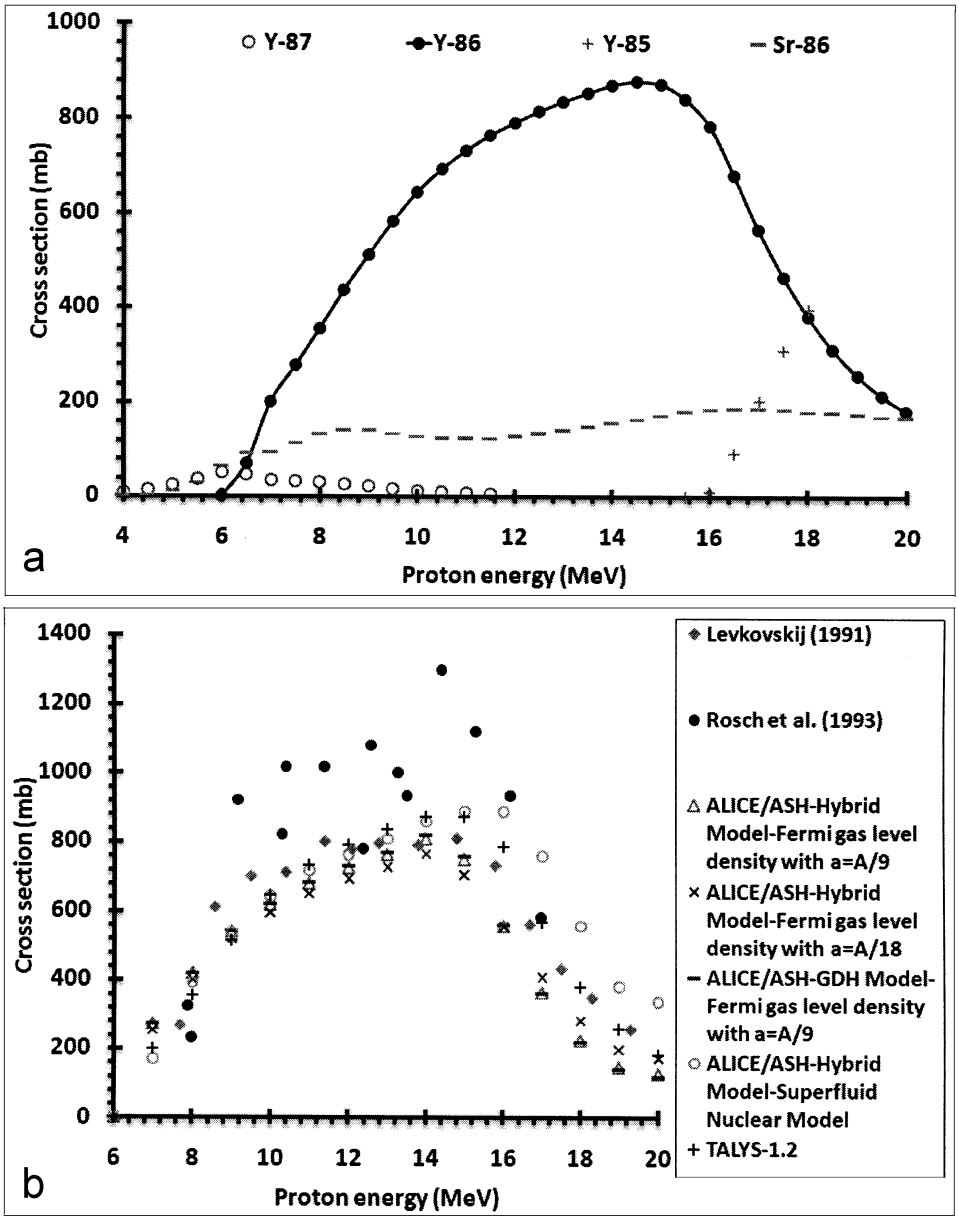

Fig. 1. Excitation function of ^{86}Sr(p,n)^{86}Y reaction (a) by TALYS-1.2 code (b) via experimental data [11], level density options of ALICE/ASH 0.1 and TALYS-1.2 codes.

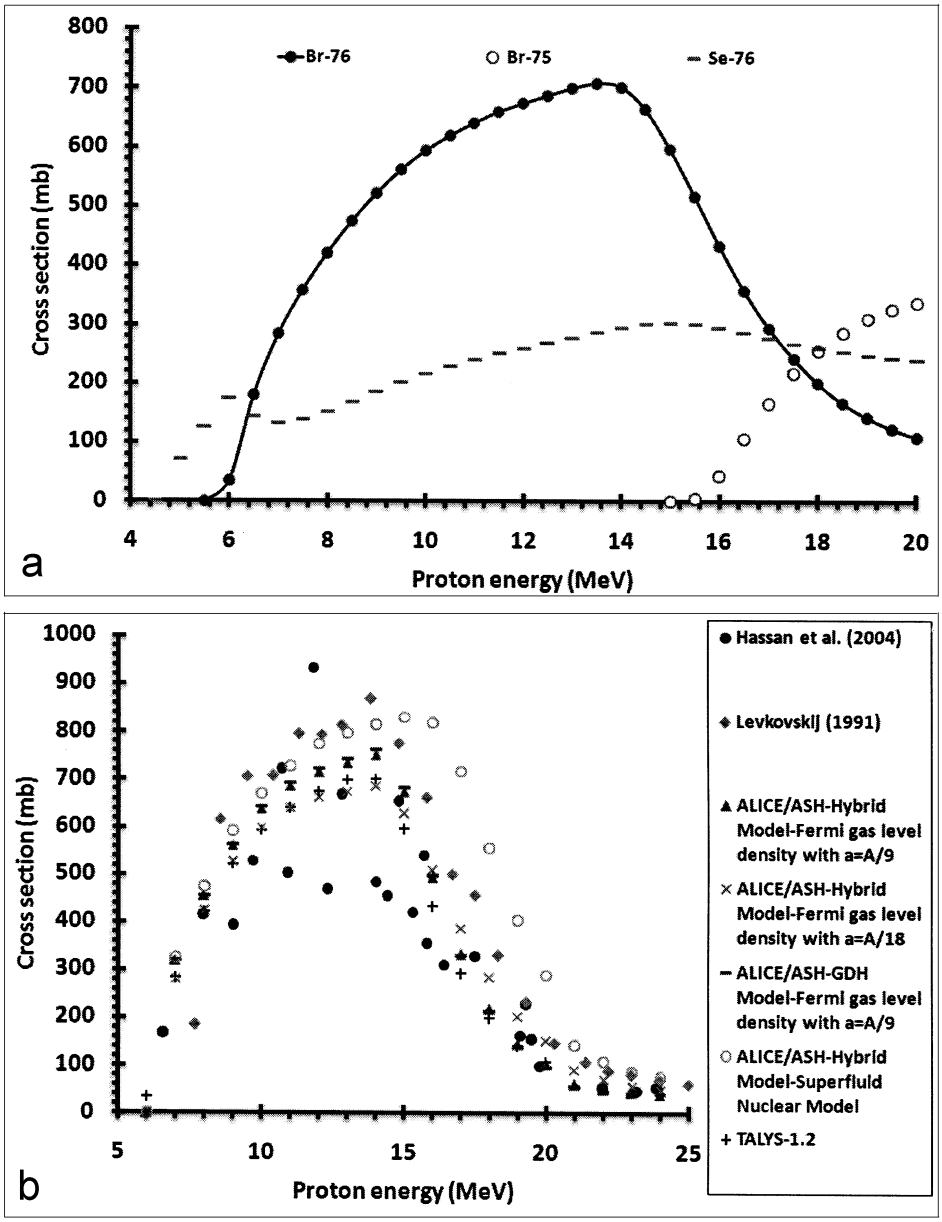

Fig. 2. Excitation function of ^{76}Se(p,n)^{76}Br reaction (a) by TALYS-1.2 code (b) via experimental data [11], level density options of ALICE/ASH 0.1 and TALYS-1.2 codes.

element, $\sigma(E)$ is the cross section at energy E, I is the projectile current, $dE/d(\rho x)$ is the stopping power, λ is the decay constant of the product and t is the time of irradiation. The production yields of positron emitters via different reactions were calculated using the Simpson numerical integral as of Eq. (29) (Table 1) [45].

Results and discussion

Excitation function of ^{86}Sr(p,n)^{86}Y reaction

Excitation functions of the proton-induced reaction on strontium-86 were measured by ALICE/ASH and TALYS-1.2 codes and compared to existing data. Figure 1 shows a comparison between calculated cross section from options of ALICE-ASH code, TALYS-1.2 code, and the experimental data that have been studied by Levkovskij [30] and Rösch *et al.* [41]. As a result, experimental data by Levkovskij are lesser than those of Rösch *et al.* Also, there is a relatively good agreement between the experimental data by Levkovskij and the prediction of the excitation function made by ALICE/ASH and TALYS-1.2 codes. The evaluation of the acquired data showed that the best range of the energy is 13 to 18 MeV. According to SRIM code the required target thickness should be 73.45 μm.

Excitation function of ^{76}Se(p,n)^{76}Br reaction

Using the ^{76}Se(p,n)^{76}Br reaction to produce ^{76}Br, the best range of incident energy was assumed 17 to 12 MeV whose maximum cross section by ALICE/ASH – hybrid model superfluid nuclear model is 831.261 mb (E_p = 15 MeV) (Fig. 2). According to SRIM code, the required target thickness should be 49 μm. The ^{76}Se(p,n)^{76}Br reaction, in the chosen range, led to form the ^{75}Br im-

purity. The separation of isotope impurities is possible by chemical methods, so this reaction is carrier free for ^{76}Br production. Over the last 15 years, this process has become the most frequently used reaction for the production of ^{76}Br. The cross sections for this reaction have been measured by Levkovskij [30] and Hassan *et al*. [13]. The nuclear model calculations (performed as for ^{76}Se(p,n)^{76}Br reaction) agree well with the measured values up to 25 MeV; but the data reported by Hassan *et al*. show strong inconsistencies; so nuclear model calculations can play an important role in removing the discrepancies.

Excitation function of ^{64}Ni(p,n)^{64}Cu reaction

According to ALICE/ASH and TALYS-1.2 codes, beneficial energy range of the projectile particle (proton) to produce ^{64}Cu from ^{64}Ni target is 13 to 8 MeV among which maximum cross section by ALICE/ASH – hybrid model Kataria-Ramamurty formula with shell corrections 812.13 mb (E_p = 11 MeV). Carrier-free ^{64}Cu production can be obtained using proton energy of less than 11 MeV. According to calculations from SRIM code the required target thickness should be 101 μm. The results of nuclear model calculations by the two codes with the measurement by Szelecsényi *et al*. [52], Avila-Rodriguez *et al*. [2] and Rebeles *et al*. [40] are shown in Fig. 3. The results of ALICE/ASH and TALYS-1.2 codes are in good agreement with the measured data from Rebeles *et al*., but experimental data by Szelecsényi *et al*. and Avila-Rodriguez *et al*. are lesser than two codes of Rebeles *et al*.

Excitation function of ^{66}Zn(p,n)^{66}Ga reaction

According to ALICE/ASH and TALYS-1.2 codes, beneficial energy range of the projectile particle (proton) to produce ^{66}Ga from ^{66}Zn target is 15 to 9 MeV among

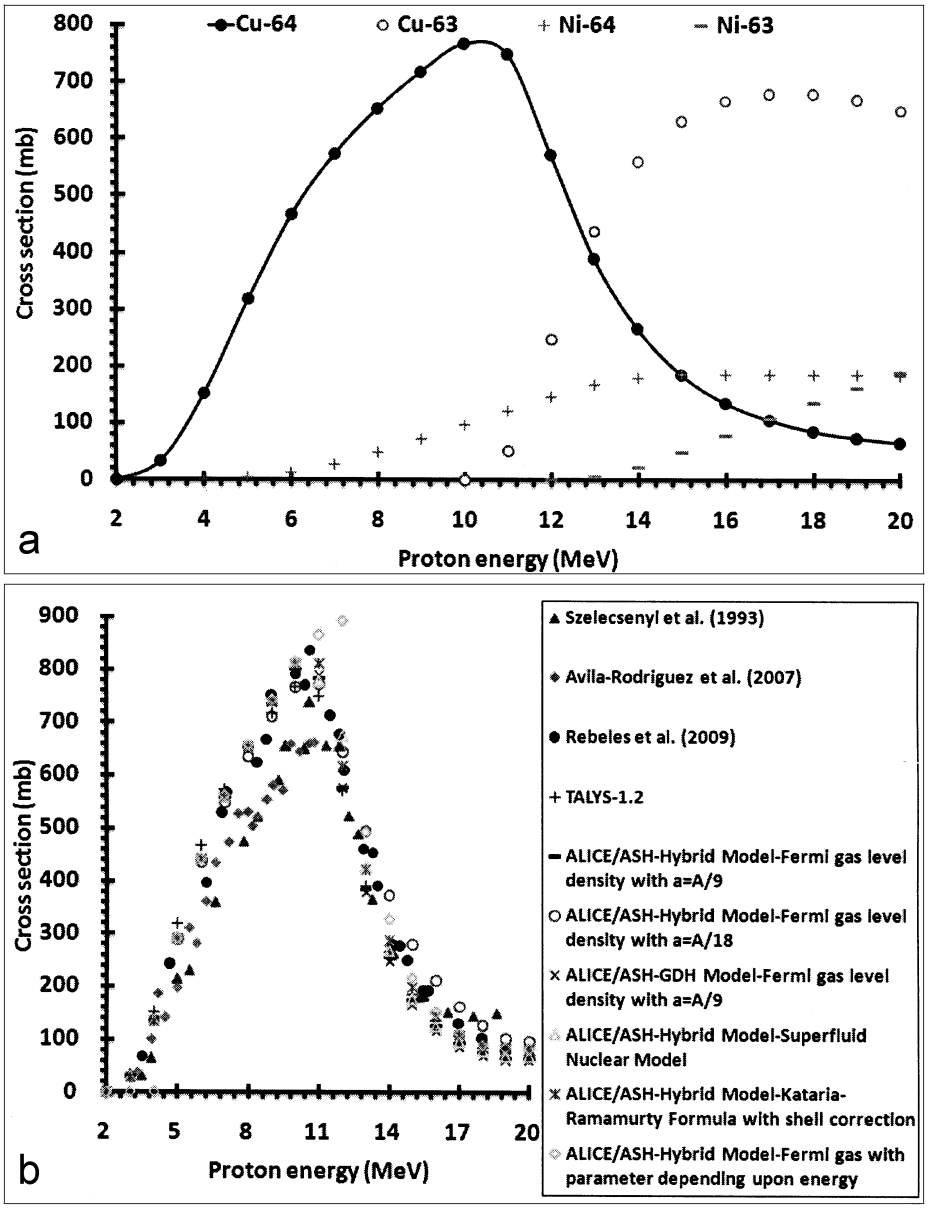

Fig. 3. Excitation function of ^{64}Ni(p,n)^{64}Cu reaction (a) by TALYS-1.2 code (b) via experimental data [11], level density options of ALICE/ASH 0.1 and TALYS-1.2 codes.

which maximum cross section by ALICE/ASH-Hybrid Model-Superfluid Nuclear Model is 683.3 mb (E_p = 13 MeV). In using ^{66}Zn(p,n)^{66}Ga reaction to produce ^{66}Ga, the best range of the incident energy was assumed to be 13 to 9 MeV. For this reaction, five cross-section measurements exist in the literature (Fig. 4). Experimental data that have been studied by Szelecsényi *et al.* [53], Hille *et al.* [16], Levkovskij [30], Little *et al.* [31] and Hermanne *et al.* [15]. Experimental data by Little *et al.* and Hermanne *et al.* are lesser than those of Szelecsényi *et al.*, Hille *et al.* and Levkovskij. ALICE/ASH code agree well with the measured data from Szelecsényi *et al.*, Hille *et al.* and Levkovskij up to 25 MeV. Also, the results of TALYS-1.2 code are in good agreement with the measured data by Hermanne *et al.*

Excitation function of ^{43}Ca(p,n)^{43}Sc reaction

Using ^{43}Ca(p,n)^{43}Sc reaction to produce ^{43}Sc, the best range of incident energy was assumed 6 to 13 MeV, the maximum cross section by TALYS-1.2 code being 394.76 mb (E_p = 9 MeV) (Fig. 5). Also maximum cross section of level density options of ALICE/ASH by Fermi gas level density ($a = A/18$) is 348.93 mb (E_p = 7.5 MeV). According to SRIM code, the required target thickness should be 220 μm. The separation of isotope impurities is possible by chemical methods, so this reaction is carrier free for ^{43}Sc production. This reaction was investigated only by de Waal *et al.* [9] and Levkovskij [30]. Experimental data and options of ALICE/ASH code are lesser than TALYS-1.2 code. De-

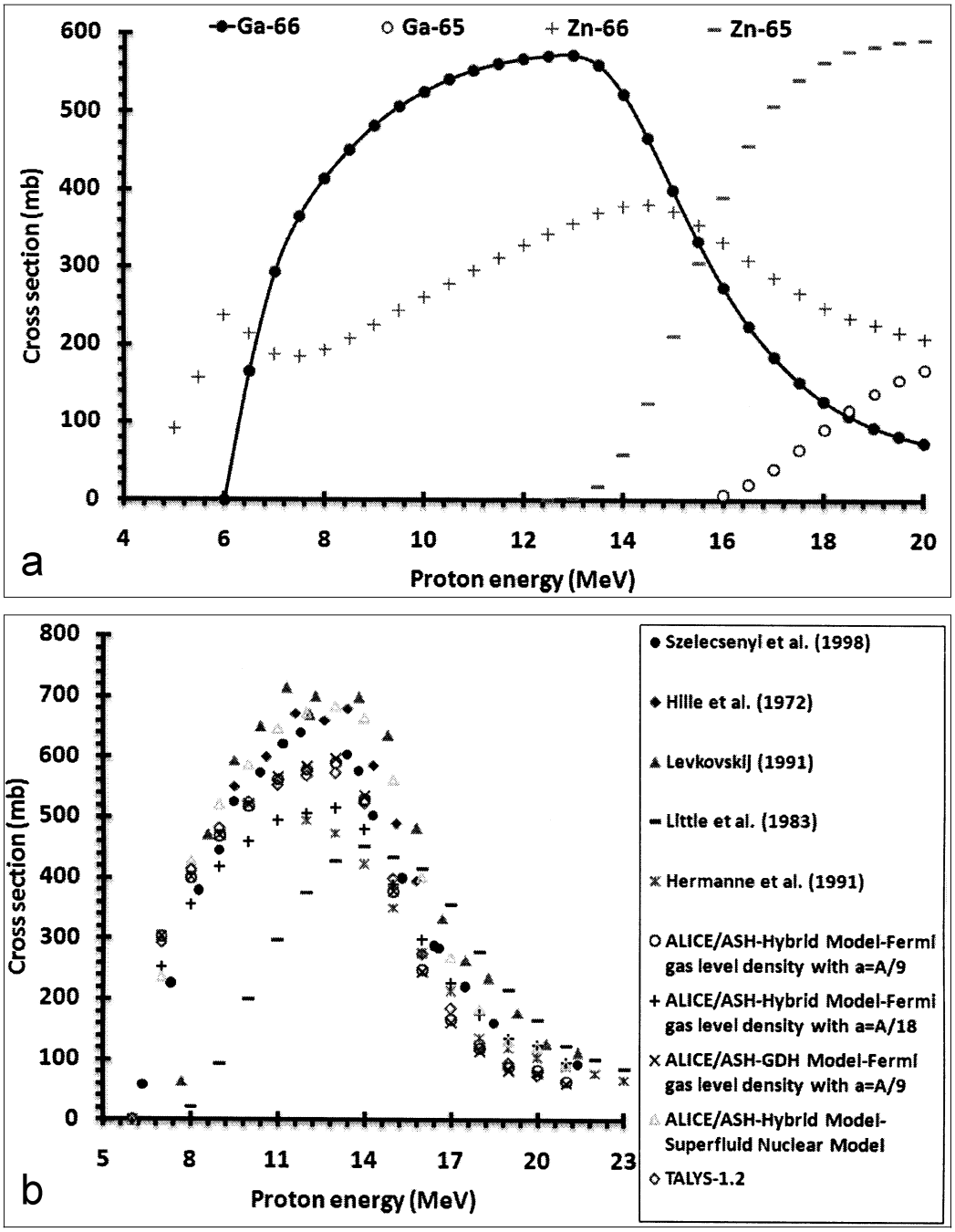

Fig. 4. Excitation function of ^{66}Zn(p,n)^{66}Ga reaction (a) by TALYS-1.2 code (b) via experimental data [11], level density options of ALICE/ASH 0.1 and TALYS-1.2 codes.

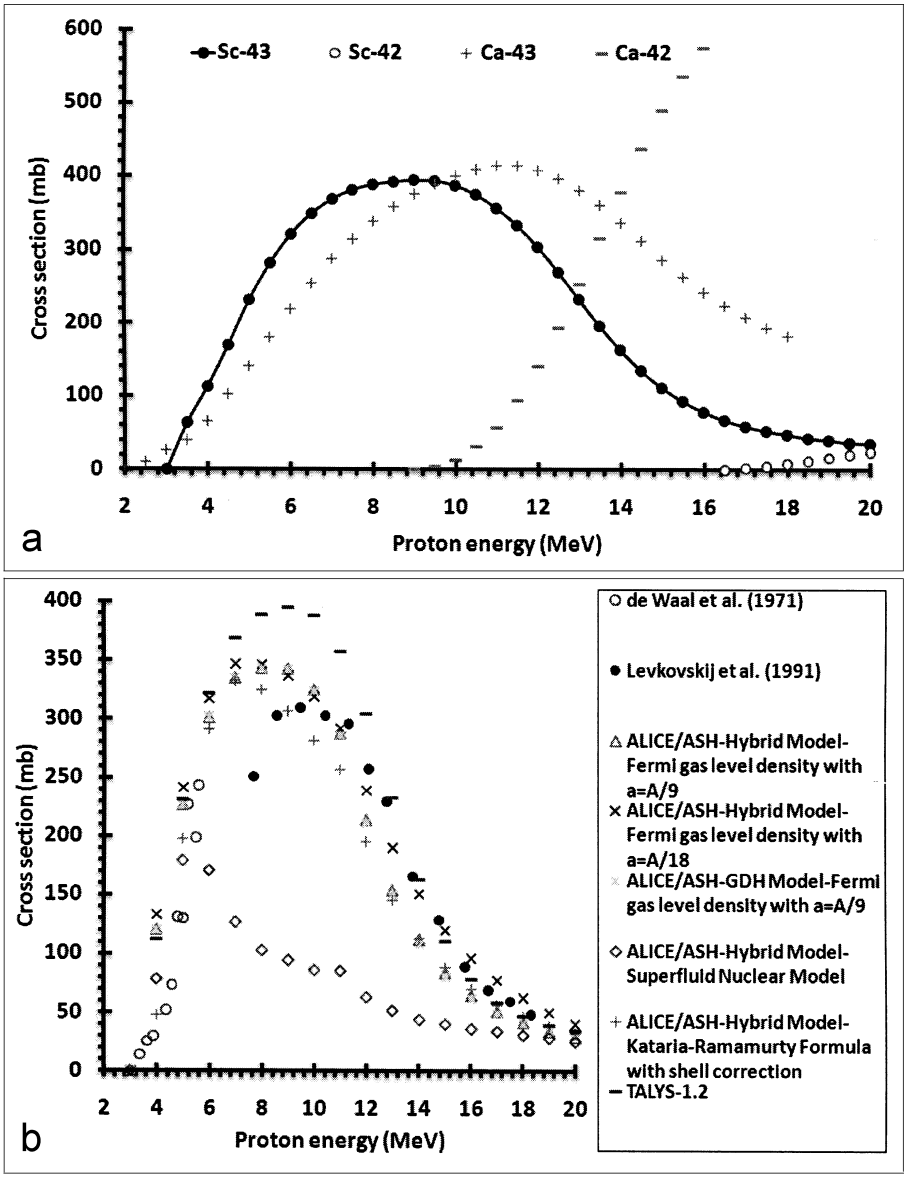

Fig. 5. Excitation function of ^{43}Ca(p,n)^{43}Sc reaction (a) by TALYS-1.2 code (b) via experimental data [11], level density options of ALICE/ASH 0.1 and TALYS-1.2 codes.

spite the existing inconsistencies among the measured cross sections, the excitation function is described well by the model calculations. The evaluated cross-section curve is also shown in Fig. 5.

Conclusions

PET is the most sensitive method to image trace amounts of molecules *in vivo*. The production of ^{86}Y, ^{43}Sc, ^{64}Cu, ^{66}Ga and ^{76}Br can be achieved by ^{86}Sr(p,n)^{86}Y, ^{43}Ca(p,n)^{43}Sc, ^{66}Zn(p,n)^{66}Ga, ^{64}Ni(p,n)^{64}Cu and ^{76}Se(p,n)^{76}Br reactions ideal reaction for low energy cyclotrons. Moreover, they are non-carrier added production feasibility using proton energy considered as a brilliant advantage.

References

1. Avila-Rodriguez MA, Nyeb JA, Nickles RJ (2007) Simultaneous production of high specific activity ^{64}Cu and ^{61}Co with 11.4 MeV protons on enriched ^{64}Ni nuclei. Appl Radiat Isot 65:1115–1120
2. Avila-Rodriguez MA, Nyeb JA, Nickles RJ (2008) Production and separation of non-carrier-added ^{86}Y from enriched ^{86}Sr targets. Appl Radiat Isot 66:9–13
3. Belgya T, Bersillon O, Capote-Noy R *et al.* (2006) Handbook for calculations of nuclear reaction data, RIPL-2. IAEA-TECDOC-1506. IAEA, Vienna, http://www-nds.iaea.or.at/RIPL-2/
4. Bethe H (1937) Nuclear dynamics, theoretical. Rev Mod Phys 9:69–244
5. Blann M (1991) ALICE-91, RSIC code, PACKAGE PSR-146. Report UCRL-JC-109052. Lawrence Livermore National Laboratory, California, USA
6. Broeders CHM, Konobeyev AYu, Korovin AYu, Lunev VP, Blann M (2006) ALICE/ASH – pre-compound and evaporation model code system for calculation of excitation functions, energy and angular distributions of emitted particles in nuclear reaction at intermediate energies, FZK 7183, http://bibliothek.fzk.de/zb/berichte/FZKA7183.pdf
7. Daube-Whiterspoon ME, Green SL, Plascjak P, Carson E, Eckelman WC (1997) RET imaging characteristics of ^{66}Ga. J Nucl Med 38:317–329

8. Demetriou P, Goriely S (2001) Microscopic nuclear level densities for practical applications. Nucl Phys A 695:95–108
9. de Waal Peisach M, Pretorius R (1971) Activation cross sections for proton-induced reactions on calcium isotopes up to 5·6 MeV. J Inorg Nucl Chem 33:2783–2789
10. Ericson T (1960) The statistical models and nuclear level densities. Adv Phys A 9:425–430
11. EXFOR/CSISRS: Experimental Nuclear Reaction Data, www-nds.iaea.org/exfor
12. Ferrari M, Cremonesi M, Bartolomei M *et al*. (2006) Dosimetric model for locoregional treatments of brain tumors with ^{90}Y-conjugates: clinical application with ^{90}Y-DOTATOC. J Nucl Med 47:105–112
13. Hassan HE, Qaim SM, Shubin Yu, Azzam A, Morsy M, Coenen HH (2004) Experimental studies and nuclear model calculations on proton-induced reactions on ^{nat}Se, ^{76}Se and ^{77}Se with particular reference to the production of the medically interesting radionuclides ^{76}Br and ^{77}Br. Appl Radiat Isot 60:899–909
14. Helisch A, Forster GJ, Reber H *et al*. (2004) Pre-therapeutic dosimetry and biodistribution of ^{86}Y-DOTA--Phe1-Tyr3-octreotide vs. ^{111}In-pentetreotide in patients with advanced neuroendocrine tumours. Eur J Nucl Med 31:1386–1392
15. Hermanne A, Walravens N, Cicchelli O (1991) Optimization of isotope production by cross-section determination. In: Qaim SM (ed) Proc of the Int Conf Nuclear Data for Science and Technology, May 1991, Jülich, Germany. Springer-Verlag, Berlin, p 616
16. Hille M, Hille P, Uhl M, Weisz W (1972) Excitation functions of (p,n) and (α,n) reactions on Ni, Cu and Zn. Nucl Phys A 198:625–640
17. Ignatyuk AV (1998) Handbook for calculations of nuclear reaction data. IAEA-TECDOC-1034. IAEA, Vienna
18. Ignatyuk AV, Istekov K, Smirenkin GN (1979) Role of collective effects in the systematics of nuclear level densities. Sov J Nucl Phys 29:450–454
19. Iwamoto A, Harada K (1982) Mechanism of cluster emission in nucleon. Phys Rev C 26:1821–1834
20. Jalilian AR, Rowshanfarzad P, Sabet M, Raisali G (2005) Preparation of [^{66}Ga]bleomycin complex as a possible PET radiopharmaceutical. J Radioanal Nucl Chem 264:617–621
21. Kataria SK, Ramamurthy VS (1978) Semiempirical nuclear level density formula with shell effects. Phys Rev C 18:549–563
22. Kataria SK, Ramamurthy VS (1980) Macroscopic systematics of nuclear level density. Phys Rev C 22:2263–2266
23. Kataria SK, Ramamurthy VS, Blann M, Komoto T (1990) Shell-dependent level densities in nuclear reaction codes. Nucl Instrum Methods A 288:585–588
24. Koning A, Hilaire S, Duijvestijn M (2005) TALYS: Comprehensive nuclear reaction modeling. Nuclear Research and Consultancy Group (NRG) Netherlands, http://www.nrg.eu/docs/nrglib/2004/koninga1.pdf
25. Koning AJ, Hilaire S, Duijvestijn M (2009) TALYS-1.2. A nuclear reaction program. User manual. Nuclear Research and Consultancy Group (NRCG) 1755 ZG Petten, Netherlands, www.talys.eu/
26. Konobeyev AYu, Korovin YuA, Lunev VP *et al.* (1992) MENDL: Activation data library for intermediate energies. Version 1. Report NDS-136. IAEA, Vienna
27. Konobeyev AYu, Korovin YuA, Pereslavtsev PE (1997) Code ALICE/ASH for calculation of excitation functions, energy and angular distributions of emitted particles in nuclear reactions. Report of the Obninsk Institute of Nuclear Power Engineering
28. Korovin YuA, Konobeyev AYu, Pereslavtsev PE *et al.* (2001) Evaluated nuclear data files for accelerator driven systems and other intermediate and high-energy applications. Nucl Instrum Methods A 463:544–556
29. Lang L, Ma Y, Kim BM *et al*. (2009) [^{76}Br]BMK-I-152, a non-peptide analogue fro PET imaging of corticotropin--releasing hormone type I receptor (CRHR1). J Lab Comp Radio 52:394–400
30. Levkovskij VN (1991) Activation cross sections for medium mass nuclei (A = 40–100) by medium energy protons and alphas particles (E = 10–50 MeV). Moscow
31. Little E, Lagunas-Solar C (1983) Cyclotron production of Ga-67. Cross sections and thick-target yields for the Zn-67(p,n) and Zn-68(p,2n) reactions. Appl Radiat Isot 34:631–637
32. Mathias CJ, Lewis MR, Reichert DE *et al*. (2003) Preparation of ^{66}Ga- and ^{68}Ga-labeled Ga(III)-deferoxamine--folate as potential folate-receptor-targeted PET radiopharmaceuticals. Nucl Med Biol 30:725–731
33. Myers WD, Swiatecki WJ (1967) Anomalies in nuclear masses. Arkiv für Fysik 36:343–352
34. Nerlo-Pomorska B, Pomorski K (2007) On the average pairing energy in nuclei. Int J Mod Phys E 16:328–336
35. Nerlo-Pomorska B, Pomorski K, Bartel J, Dobrowolski A (2008) Nuclear level density parameter. Acta Phys Pol B 39:417–420
36. Obata A, Kasamatsu S, McCarthy DW *et al*. (2003) Production of therapeutic quantities of ^{64}Cu using a 12 MeV cyclotron. Nucl Med Biol 30:535–539
37. Qaim SM (2003) Cyclotron production of medical radionuclides. In: Vértes A, Nagy S, Klencsár Z (eds) Handbook of nuclear chemistry. Kluwer, Dordrecht. Vol. 4, pp 47–76
38. Qaim SM (2008) Decay data and production yields of some non-standard positron emitters used in PET. Quar J Nucl Med Mol Imag 52:111–120
39. Qaim SM, Bisinger T, Hilgers K, Nayak D, Coenen HH (2007) Positron emission intensities in the decay of ^{64}Cu, ^{76}Br and ^{124}I. Radiochim Acta 95:67–73
40. Rebeles RA, van den Winkel P, Hermanne A, Tárkányi F (2009) New measurement and evaluation of the excitation function of ^{64}Ni(p,n) reaction for the production of ^{64}Cu. Nucl Instrum Methods B 267:457–461
41. Rösch F, Qaim SM, Stöcklin G (1993) Nuclear data relevant to the production of the positron emitting radioisotope ^{86}Y via the ^{86}Sr(p,n) and ^{nat}Rb(^{3}He,xn) processes. Radiochim Acta 61:1–8
42. Rowshanfarzad P, Jalilian AR, Sabet M, Akhlaghi M (2004) Production and quality control of ^{66}Ga as a PET radioisotope. Ir J Radiat Res 2:149–158
43. Sadeghi M, Amiri M, Roshanfarzad P, Avila M, Tenreiro C (2008) Radiochemical studies relevant to the no-carrier--added production of $^{61/64}$Cu at a cyclotron. Radiochim Acta 96:399–402
44. Sadeghi M, Amiri M, Rowshanfarzad P, Gholamzadeh Z, Ensaf M (2008) Thick zinc electrodepositionon copper substrate for cyclotron production of ^{64}Cu. Nukleonika 53:155–160
45. Sadeghi M, Enferadi M, Nadi H (2010) Study of the cyclotron production of ^{172}Lu: an excellent radiotracer. J Radioanal Nucl Chem (in press)
46. Sadeghi M, Zali A, Sarabadani P, Aslani G, Majdabadi A (2009) Targetry of $SrCO_3$ on a copper substrate by sedimentation method for the cyclotron production of no-carrier-added ^{86}Y. Appl Radiat Isot 67:2029–2032
47. Sadeghi M, Zali A, Zeinali B (2009) ^{86}Y production via ^{86}Sr(p,n) for PET imaging at a cyclotron. Appl Radiat Isot 67:1393–1396
48. Sato K, Iwamoto A, Harada K (1983) Pre-equilibrium emission of light composite particles in the framework of the exciton model. Phys Rev C 28:1527–1537

49. Shubin YuN, Lunev VP, Konobeyev AYu (1995) International codes and model intercomparison for intermediate energy. Report Institute of Physics and Power Engineering (IPPE), Obninsk, N2461
50. Spahn I, Steyn GF, Vermeulen C *et al*. (2009) New cross-section measurements for production of the positron emitters ^{75}Br and ^{76}Br via intermediate energy proton induced reactions. Radiochim Acta 97:535–541
51. Strutinsky VM (1958) Proceedings of the International Congress on Physics of Nuclear Application, Paris 1958, p 617
52. Szelecsényi F, Blessing G, Qaim SM (1993) Excitation functions of proton induced nuclear reactions on enriched ^{61}Ni and ^{64}Ni: possibility of production of no-carrier-added ^{61}Cu and ^{64}Cu at a small cyclotron. Appl Radiat Isot 44:575–580
53. Szelecsényi F, Boothe TE, Takács S, Tárkányi F, Tavano E (1998) Evaluated cross section and thick target yield data bases of Zn + p processes for practical applications Appl Radiat Isot 49:1005–1032
54. Tolmachev V, Stone-Elander S (2010) Radiolabelled proteins for positron emission tomography: pros and cons of labelling methods. Biochim Biophys Acta 1800:487–510
55. Zhou D, Sharp TL, Fettig NM *et al*. (2008) Evaluation of a bromine-76-labeled progestin 16α,17α-dioxolane for breast tumor imaging and radiotherapy: in vivo biodistribution and metabolic stability studies. Nucl Med Biol 35:655–663
56. Zhuravlev BV, Lychagin AÀ, Titarenko NN (2006) Nuclear-level densities around Z = 50 from neutron evaporation spectra in (p,n) reactions. Phys Atom Nucl 69:363–370
57. Ziegler JF, Biersack JP, Littmark U (2001) The stopping and range of ions in mater, SRIM code. USA, http://www.srim.org/